Energy & Buildings 359 (2026) 117295

Contents lists available at ScienceDirect

Energy & Buildings

journal homepage: www.elsevier.com/locate/enb

Elastomeric panels with Phase Change Material for summer thermal management: Experimental thermal performance in a real wall design

Maja Danovska [a,*], Francesco Valentini [b,*], Maurizio Grigiante [a], Luca Fambri [b], Andrea Dorigato [b], Alessandro Prada [a], Alessandro Pegoretti [b]

[a] University of Trento, Department of Civil, Environmental and Mechanical Engineering, Via Mesiano, 77 - 38123 Trento, Italy
[b] University of Trento, Department of Industrial Engineering and INSTM Research Unit, Via Sommarive, 9 - 38123 Trento, Italy

ARTICLE INFO

Keywords:
Thermal load management
Phase Change Materials (PCMs)
Building envelope
Decrement factor
Time-shift
Dynamic thermal performance

ABSTRACT

This study investigates the integration of elastomeric panels containing Phase Change Materials (PCMs) into real-scale building wall assemblies to improve their transient thermal performance. PCMs offer a promising passive strategy to enhance thermal inertia and reduce cooling loads by absorbing and releasing latent heat during phase transitions. Despite their potential, their performance in real-world wall configurations under dynamic boundary conditions remains insufficiently explored. To address this gap, three wall systems were experimentally tested: a reference wall (made up of fruit processing organic by-products), the same wall with a 5 mm PCM layer, and with a 10 mm double PCM layer. Tests were conducted using a double climatic chamber to simulate real daily temperature profiles based on standard sinusoidal conditions and representative summer climates of Trento and Palermo (Italy). Key dynamic thermal parameters, including periodic thermal transmittance, decrement factor, and time-shift, were evaluated along with the thermal capacitance. Results showed that 5 mm PCM integration substantially improved the wall thermal behaviour: the periodic thermal transmittance was decreased from 1.1 to 0.4 W m^{-2} K^{-1}, the time shift was increased from 2.8 to 6.7 h, the decrement factor was reduced from 0.72 to 0.29 and the energy stored in a daily cycle was increased from 247 to 427 Wh m^{-2}. The 10 mm PCM configuration reduced the peak of the internal heat flux by up to 64.6% and increased time-shift of the reference wall by over 130% under sinusoidal forcing. Additionally, stored thermal energy increased by over 70% compared to the reference wall. The evaluation of the energy and thermal power implication of the PCM integration revealed the possibility of size reduction of HVAC system due to the lower peak demand.

1. Introduction

The building sector, including both services and residential buildings, accounts for nearly 40% of final energy consumption, of which more than 50% is related to space heating and cooling [1–4]. The increasing frequency of heat waves and the intensification of the urban heat island effect have significantly raised cooling demand in warm and Mediterranean climates, where air conditioning alone can represent up to 60% of total energy use [5,6]. Given the Mediterranean basin's high vulnerability to climate change and the projected rise in temperatures [5,7], this trend is expected to worsen in the coming decades. Moreover, even Alpine climate regions, traditionally characterized by cooler temperatures, are now increasingly experiencing extreme heat events. Recent studies [8] identify the Alpine region as a hot spot of global warming, with above-average warming rates and growing exposure to heat waves. Therefore, improving the thermal performance of building envelopes is a key strategy to meet net-zero emissions targets in the building sector by 2050 [9]. According to the EU's energy transition roadmap, thermal energy storage systems will play a central role in achieving these goals [10–12]. Latent heat storage using phase change materials (PCMs) is one of the most promising solutions in this context [13]. Paraffin-based PCMs are particularly attractive due to their high latent heat, low cost, and long-term chemical stability [14]. These materials store and release latent heat during solid–liquid transitions, helping to regulate indoor temperatures by reducing thermal fluctuations and shifting peak loads. As a result, PCMs have been integrated into various construction materials and systems, including concrete [15–18], bricks [19,20], mortars [21–23], walls [24], gypsum boards, floors [25,26], roofs [27], and windows [28].

Despite their promising potential, several challenges limit the widespread adoption of PCMs in real constructions. First, the accurate

* Corresponding authors.
E-mail addresses: maja.danovska@unitn.it (M. Danovska), francesco.valentini@unitn.it (F. Valentini).

https://doi.org/10.1016/j.enbuild.2026.117295
Received 17 December 2025; Received in revised form 22 February 2026; Accepted 8 March 2026
Available online 10 March 2026

Nomenclature

Symbols

Δq	Heat flux variation (external − internal) ($W \cdot m^{-2}$)
Δt_{ie}	Time-shift (h)
E	Stored energy ($Wh \cdot m^{-2}$)
f	Decrement factor (−)
q	Heat flux ($W \cdot m^{-2}$)
R	Thermal resistance ($m^2 \cdot K \cdot W^{-1}$)
U	Thermal transmittance (U-value) ($W \cdot m^{-2} \cdot K^{-1}$)
Y_{ie}	Periodic thermal transmittance ($W \cdot m^{-2} \cdot K^{-1}$)

Acronyms

EPDM	Ethylene Propylene Diene Monomer
FFT	Fast Fourier Transform
HVAC	Heating, Ventilation, and Air Conditioning
NBR	Nitrile Butadiene Rubber
oMMT	Organo-modified Montmorillonite
PA	Palermo
PCM	Phase Change Material
PCM1	Wall with single 5 mm PCM layer
PCM2	Wall with double 5 mm PCM layer (10 mm total)
REF	Reference wall
STD	Standard sinusoidal forcing
TN	Trento

determination of PCM thermophysical properties remains a critical task for representative modelling and suitable application [29]. Second, there is a lack of effective, scalable, and validated strategies for integrating PCMs into building envelopes [30–35]. Most existing studies rely on numerical simulations [13,27,36–45] or small-scale setups under idealized boundary conditions [15,18,40,44], which limits their relevance for real-world applications. Although much of the literature relies on simulations, several studies have examined PCM performance in buildings at bigger scale. Specifically, Athienthis et al. [26] tested PCM wallboards integrated in a passive solar room and observed a reduction of indoor peak temperature by approximately 4 °C, with marked heating load reductions during the night. Cabeza et al. [18] evaluated microencapsulated PCM in concrete walls of a test building in Spain, reporting a 1 °C drop in maximum indoor temperature and a 2-hour shift in the peak load. In Portugal, Figueiredo et al. [41] monitored some walls integrated with PCMs in real occupied university building and they demonstrated that overheating could be prevented under summer conditions. However, they highlighted the necessity of a sufficient ventilation during the night in order to allow to the PCM the solidification phase. Guarino et al. [46] investigated a south-facing PCM wall in Montreal, showing heating and cooling load reductions of 17% and 20% in cold climates. Similarly, Ye et al. [47] carried out full-scale experiments in China using test rooms, confirming that PCM integration can improve comfort by reducing indoor temperature fluctuations but such result varied seasonally.

Even though several studies have examined PCM under real conditions, the existing literature remains limited and inconsistent and therefore insufficient to provide strong evidence of the efficiency of the approach [35,48,49]. In addition, there is a lack of a systematic and reproducible methodology, which limits the widespread of technical results and the knowledge related to PCMs. For instance, when focusing on scale and realism, works are considering either oversimplified conditions with small test modules not representing the real building behaviour [26], or extremely complex situations like in real occupied buildings [41] whose results are hard to generalize. Regarding the climate-dependency, studies show to be extremely location-specific with different test configurations adopted under different climates, limiting the investigation of climate-dependent PCM behaviour [34,49]. Therefore, these factors do not allow a direct comparison of research outcomes. Moreover, a comprehensive review by Ahmad et al. [35] emphasized the fragmentation of current PCM research, identifying the lack of combined thermal and economic evaluation in real construction contexts as an important limitation to practical implementation.

This work presents a comprehensive experimental investigation of elastomeric PCM panels integrated into real-scale wall assemblies, evaluated under realistic, dynamic thermal conditions using a double climatic chamber. The study advances the field in several ways. Firstly, it provides an experimental evaluation of dynamic thermal behaviour, including periodic thermal transmittance, decrement factor, and time-shift, for real wall systems exposed to daily temperature cycles representative of both temperate and warm Mediterranean climates. While some previous studies reported dynamic metrics, few focused on bigger scale components or climate-specific variations. Secondly, this research explicitly investigates the performance limitations of PCMs in different climates, especially in warmer ones where latent heat cycling may be suppressed by persistently high ambient temperatures, which is an aspect not sufficiently analysed [15,27]. Thirdly, the study investigates the energy and thermal power implications of PCM integration in building walls that quantifies the impact of PCM layers on HVAC peak load reduction and system sizing, directly addressing the economic feasibility gap [35]. This contribution collectively aims to support the scalable, climate-depending integration of PCM technologies in energy-efficient buildings, and to guide their practical adoption in both new constructions and retrofit scenarios.

2. Materials and methods

2.1. Test cases

The experimental study examined three wall configurations (Fig. 1): (i) a reference wall (REF) measuring 1000 mm × 1200 mm × 250 mm, made of hollow bricks from organic residues with external clay finishes. (ii) A second setup (PCM1) using the reference wall plus a 5 mm-thick phase change material layer on the external surface, assembled from multiple panels joined with thermal insulation tape. (iii) A third configuration (PCM2) featuring the reference wall with a 10 mm-thick PCM layer (double layer: 5 + 5 mm) on the exterior. The choice of the PCM thicknesses came from the manufacturing process, in particular the vulcanization process during which a single panel was made with a thickness of 5 mm, while the double layer with 10 mm thickness was achieved by stacking two panels together. This allowed a controlled investigation of how increasing PCM mass and thermal inertia influences time lag, decrement factor, and energy storage capacity. Elastomeric panels, whose detailed preparation, pictures and characterization are reported in [50,51], consisted of an Ethylene-Propylene Diene Monomer) (EPDM) matrix containing paraffin RT28HC[1] premixed with an organo-modified montmorillonite (oMMT), and enclosed in an external envelope made of Nitrile Butadiene Rubber (NBR) rubber to avoid paraffin leakage. The PCM content in the composite was equal to 56 wt%, leading to a melting enthalpy of 96.7 J g^{-1} with a melting peak at 25.1 °C, a thermal conductivity of 0.11 W $m^{-1} \bullet K^{-1}$ (at 10 °C) and a specific heat capacity of 2.15 J $g^{-1} \bullet K^{-1}$ (at 5 °C) [50,51]. A multilayer wall composed of two layers of clay plaster and a patented hollow brick made from organic residues was used as the reference system for the PCM insulation. This configuration was selected to replicate typical existing structures while incorporating an innovative

[1] The main thermal properties from the technical data sheet are: melting point 28 °C, melting enthalpy 250 J g^{-1}, specific heat capacity 2 kJ $kg^{-1} \bullet K^{-1}$, thermal conductivity of 0.2 W $m^{-1} \bullet K^{-1}$. The melting temperature measured through differential scanning calorimetry at 1 °C min^{-1} is equal to 24.5 °C with an associated melting enthalpy of 262.9 J g^{-1} [51,62].

Fig. 1. Tested walls.

material with a low life-cycle impact.

2.2. Experimental setup

A double-climatic chamber was used to impose controlled ambient conditions on both sides of the tested walls (Fig. 2). The instrument consists of two independent chambers both equipped with electric resistances and refrigeration plants for the heating/ cooling cycles and control systems to ensure desired boundary conditions. The air circulation systems present inside both chambers ensure a uniform temperature on both sample surfaces.

Experimental measurements were gathered by a Data Acquisition System, composed of temperature probes, heat flux meters and a logger, required for the monitoring of the tested sample under the different test conditions. At the external and internal sides of all the three walls, temperature thermal resistances (± 0.24 °C accuracy, coverage factor equal to 1.96) were adopted to monitor the surface temperature. Sensors were placed in the central portion of the sample (the measurement area), where edge effects are reduced. Heat flux meters (30 cm x 30 cm) with a ± 7% accuracy was installed in the central part of both surfaces to measure the heat transfer between the two chambers, as well. T-type thermocouples (± 1.07 °C accuracy, coverage factor equal to 1.96) and heat flux meters with a lower dimension (i.e., 10 cm x 10 cm) with accuracy equal to ± 7% were installed to monitor the uniformity over the whole surface. Additional thermocouples and heat flux meters (10 cm x 10 cm) were installed to monitor the temperature and the heat transfer between layers between the reference wall and the PCM layer for the case (ii) and (iii). The logging system consists of a Keysight model DAQ970A with measurement accuracy equal to ± 0.0011% (range 100 mV) for the voltage measurement and ± 0.012% (range equal to 100 Ω) for the electrical resistance measurement. Fig. 3 represents the layout of the Data Acquisition System, respectively for each measurement surface (front view and longitudinal cross-section).

All sensors were previously calibrated to ensure an accurate monitoring of walls status. Both data regarding the environmental parameters of the two chambers and the monitored quantities of the tested samples

Fig. 2. Double climatic chamber at the Sustainable Energy Lab (University of Trento, Italy).

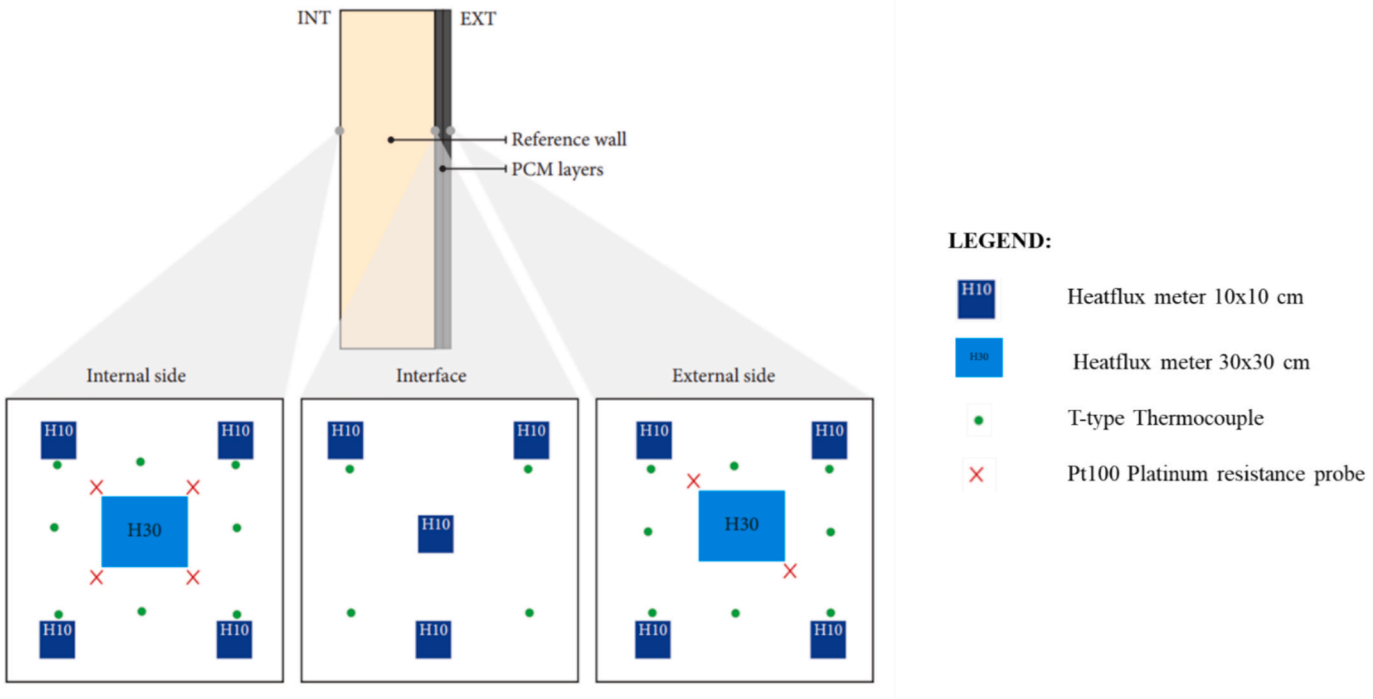

Fig. 3. Layout of the installed sensors.

were recorded every 15 min for the chamber and every 1 min time-step for the tested wall, respectively.

2.3. Experimental activities

The experimental campaign included either tests in a steady state condition and a stabilized periodic regime. Firstly, a stationary test was run to assess the thermal resistance of the wall according to the standard EN ISO 1934 [52]. This allowed a more univocal analysis of the effect of the PCM layers. The test was set by keeping the internal air temperature equal to 25 °C and the external one equal to 5 °C and air velocities were set equal to 1 m s^{-1} (indoor chamber) and equal to 2 m s^{-1} (external chamber) to ensure a proper convective heat transfer at the surface. The choice of the air velocities, particularly the indoor one, was driven by the need to ensure uniform and well-controlled convective boundary conditions, minimize thermal stratification, and improve the repeatability of the thermal measurements. Following on from this point, the external temperature was varied according to three different temperature profiles (Fig. 4), while maintaining a constant internal temperature. The first forcing profile (called STD) followed a 24-hour sinusoidal cycle with an average temperature of 25 °C and a semi-amplitude of 10 °C. The temperature in the internal chamber was kept at a constant

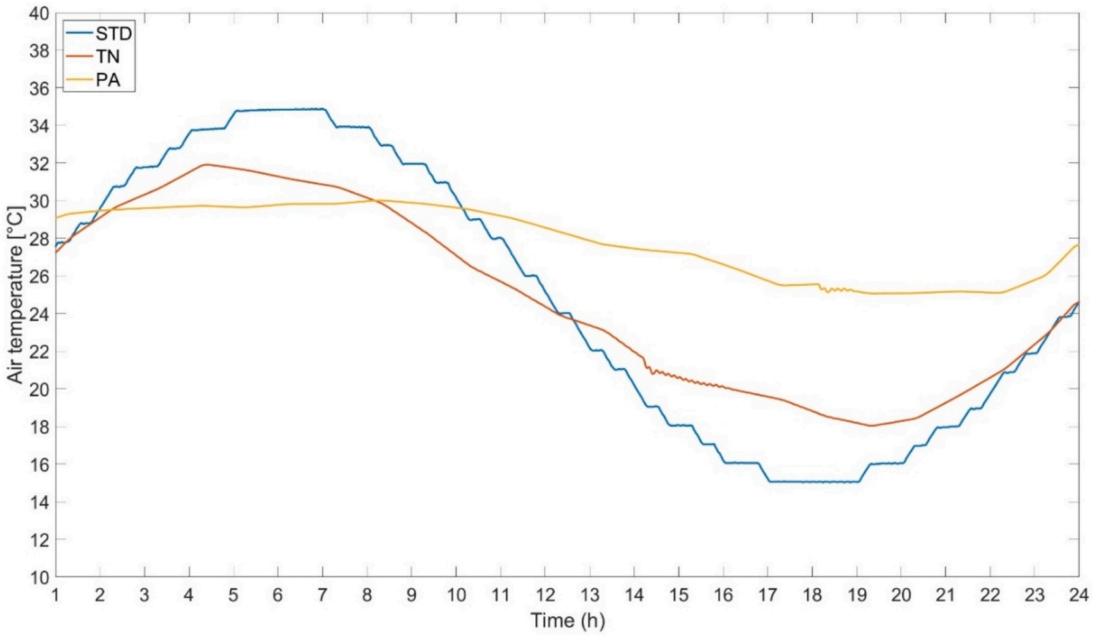

Fig. 4. Forcing temperatures applied in the external chamber.

temperature (i.e. 25 °C) to experimentally assess only the periodic response of the wall and not the constant heat flux resulting from an average temperature gradient across the wall. The other two forcing profiles were identical to those applied in the previous study [50] to allow a comparison between previous studies on PCMs on a smaller scale. These profiles represent the hourly temperatures for the cities of Trento, named as TN, and Palermo, called PA, respectively a mixed humid and warm humid climate according to ASHRAE standard 196. These profiles were derived from real climatic measurements and correspond to representative daily temperature cycles obtained from the hottest week of the year (second week of July 2022). The hourly temperature data were averaged over the seven-day period to generate a representative 24-hour profile, which was subsequently reproduced in the climatic chamber using discrete temperature steps of 1-hour duration. The adoption of average hourly values allowed the definition of realistic and repeatable thermal boundary conditions representative of extreme summer scenarios. These temperature profiles were adopted from a previous study [50] conducted on the same PCM at a smaller scale and were used here as a reference to ensure methodological consistency, representativeness of real operating conditions, and comparability between experimental results obtained at different scales. Finally, wind speed was set equal to 1.5 m s^{-1} at the internal chamber and 2 m s^{-1} at the external one to allow a uniform heat transfer on the whole surface.

Tests were run until thermal balance was reached, especially for the stationary test, while for the periodic ones, until the periodic response was not stable in each period.

2.4. Thermal performance analysis

Different thermal performance parameters were computed starting from the measured variables, namely temperature and heat flux at the surface and interfaces. Specifically, the periodic thermal transmittance (Y_{ie}), the decrement factor (f) and the time-shift (Δt_{ie}) were computed following the Standard EN ISO 13786 [53] definition to assess the summer performance of the test cases with and without PCM layers. In addition, the thermal transmittance U of each wall's configuration was computed from experimental results according to the indications of Standard EN ISO 6946 [54]. An error analysis was performed by considering the uncertainty on the single measured variable and propagating it to the performance indexes according to [55].

Moreover, assessing energy balance is essential for ensuring the effectiveness of PCM thermal performance and optimizing thermal management solutions. Knowing the heat stored during melting and released during solidification allows to understand the efficacy of the proposed passive solution. Heat flux variation (Δq) was computed taking the difference between the external (q_e) and the internal (q_i) heat flux for all tested walls (eq. (1)).

$$\Delta q = q_e - q_i \tag{1}$$

By considering each cycle and by integrating only the positive heat flux variation as function of time it is possible to compute the stored energy, named E per each cycle (Wh m^{-2}):

$$E = \frac{\int_0^t \Delta q^+ \cdot dt}{60} \tag{2}$$

with Δq computed every minute and the time t expressed in min. The stored energy was computed not only for one single stabilized period, but for all test periods. Once stabilization was reached, the stored energy was obtained as an average of the stored energy for each stabilized period.

3. Results and discussion

In this section, the results of the reference wall analysis, as well as of the wall coupled with 5- and 10-mm layer of PCM are presented in terms of both stationary and periodic thermal parameters. The stationary parameters reflect the steady-state conditions (typical of a winter performance), while the periodic parameters describe the time-dependent or cyclic variations observed. Both sets of parameters are fundamental in understanding the complete thermal behaviours of the analysed wall configurations.

3.1. Thermal characterization of the reference wall

The reference wall composed of hollow bricks from organic residues with external clay finishes was firstly characterized from the steady-state point of view, by measuring its U-value yielding a value equal to 1.239 ± 0.041 W m^{-2} K^{-1}. This reference configuration was intentionally designed with low-to-moderate thermal resistance to provide a sensitive baseline for evaluating the relative contribution of the PCM layer. In fact, highly insulated, code-compliant envelopes already ensure low steady-state and periodic thermal transmittance values, making the additional effect of PCM less relevant and more difficult to quantify. Moreover, the reduced amplitude of dynamic heat flux through highly insulated walls would partially mask the PCM contribution under laboratory conditions. For this reason, a representative low/medium-thermal resistance wall, also typical of existing Italian buildings [56], was selected to enhance the sensitivity of the measurements and enable a clearer assessment of the PCM influence in the stabilized periodic regime. Afterwards, three experiments were performed under periodic boundary conditions using different external temperature profiles. For each one, results were analysed using both the original recorded data and a filtered version of the original signal obtained by using a Fast Fourier Transform (FFT)-based harmonic decomposition function in MATLAB (v.2022) environment [57]. As regards the filtering process of the original signal, the time series was first transformed into the frequency domain using the *fft* function [57]. The DC (direct current) component or mean value and the fundamental 24-h harmonic corresponding to the daily excitation frequency were kept, while all higher-order harmonics were set to zero. The filtered signal was then reconstructed through the inverse transform (*ifft*) to obtain a waveform representing only the dominant daily periodic behaviour. This procedure is not just a conventional denoising process, rather, it isolates the fundamental harmonic component used for the evaluation of periodic thermal properties (e.g., periodic thermal transmittance, time-shift and decrement factor), consistently with the standard harmonic method. This approach improves the signal-to-noise ratio, as well as the estimation of the thermal parameters. This is consistent with the fact that walls themselves act as a low-pass filter.

Fig. 5 shows the different impact of the applied forcing inputs both on the magnitude of the transmitted heat-flux peak and on the varying trends of the heat fluxes themselves, thus highlighting the different operating conditions of the wall. For the Palermo case, since the internal temperature was higher than the external average, the heat flux did not oscillate around zero but had a mean value of approximately 4 W m^{-2}. This, however, did not affect the determination of periodic thermal parameters. Regardless of the forcing profile, the fundamental frequency remained unchanged due to the fixed periodicity of the signals.

As a result, periodic parameters such as periodic thermal transmittance, decrement factor, and time shift were similar across tests. The values of periodic thermal transmittance were comparable across all three profiles, within uncertainty intervals. The decrement factor showed the same consistency. Time shift varied more noticeably due to noise in the original data, affecting peak identification, but after signal filtering, all time shift values converged to around 2.8 h. Table 1 summarizes these results for both original and filtered signals.

3.2. Impact of a single layer of Phase Change Material

By installing an external PCM layer with 5 mm thickness to the

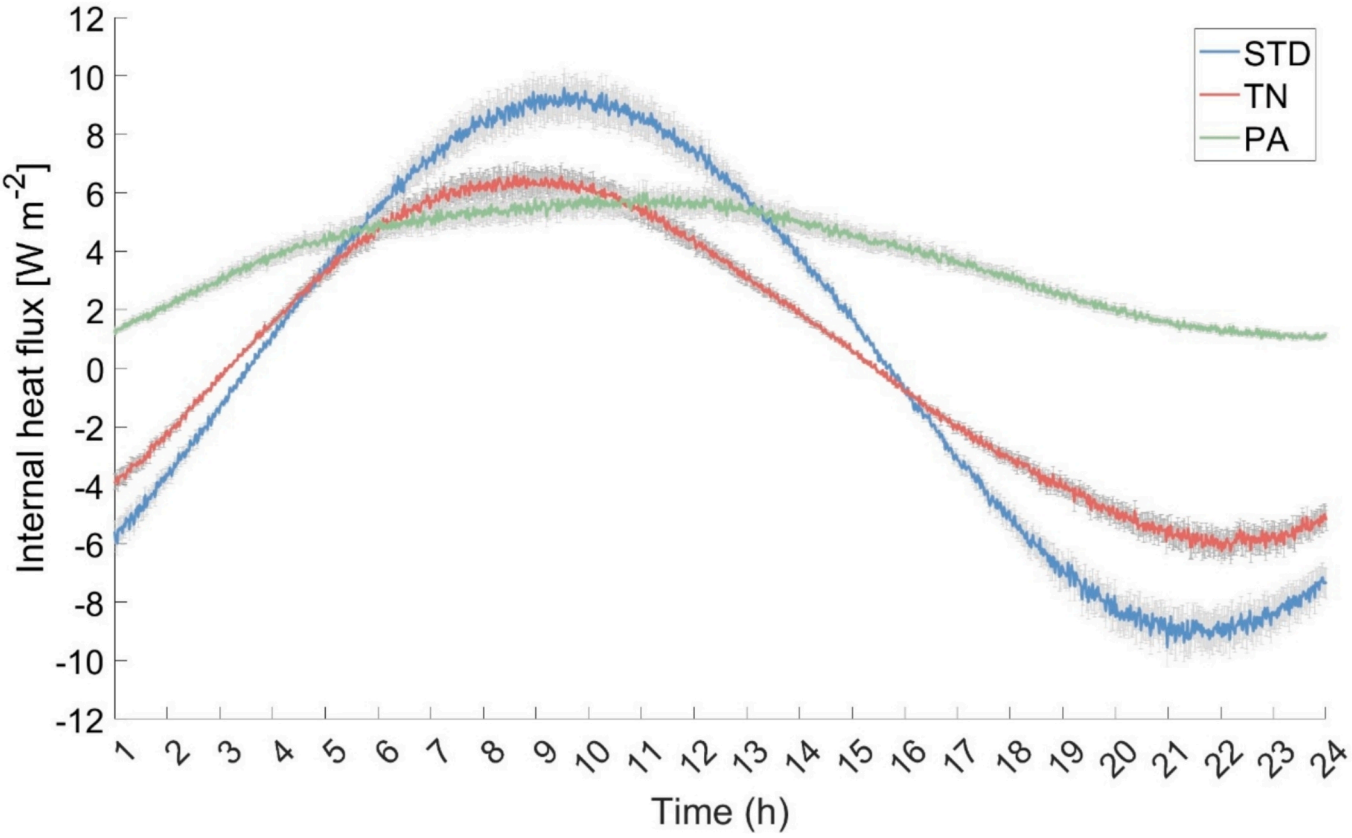

Fig. 5. Measured internal heat flux of the reference wall, considering three temperature forcing. Positive heat flux means inwards towards the internal chamber (as an indoor heat gain).

Table 1
Periodic thermal parameters obtained from original signal and filtered one.

	STD			TN			PA		
	Original		Filtered	Original		Filtered	Original		Filtered
Y_{ie} (W m^{-2} K^{-1})	1.167	(±14.1%)	1.131	1.157	(±14.4%)	1.124	1.243	(±17.9%)	1.118
Δt_{ie} (h)	2.2	(±0.8%)	2.8	3.4	(±0.6%)	2.8	3.2	(±0.6%)	2.9
f (−)	0.744	(±11.4%)	0.721	0.737	(±11.5%)	0.717	0.792	(±14.8%)	0.713

reference wall, the obtained U-value of the resulting wall was equal to 1.190 ± 0.039 W m^{-2} K^{-1}, with a reduction of 4% with respect to the reference wall. By focusing on the periodic thermal performance, the effect of integrating a 5 mm Phase Change Material layer on the external surface of a reference wall was evaluated, as well. Results related to this case were named PCM1. Key metrics included internal surface temperature, internal heat flux, and thermal storage capacitance. Fig. 6 presents the internal surface temperature and internal heat flux for all three cases, both with and without the PCM layer.

The internal surface temperatures remained largely unchanged by the PCM insertion across all scenarios, mainly due to the presence of an active indoor climate control system, which minimized the observable influence of PCM-related thermal damping. Minor temperature-shift effects were noticed, particularly under standard conditions (STD) and the Trento case (TN), and thus not statistically significant (within measurement's uncertainty equal to ± 0.24 °C). However, internal heat flux trends showed a clear influence of the PCM layer. In all conditions, the PCM consistently reduced the peak heat flux and introduced time delays, demonstrating improved energy flow regulation. For instance, under STD forcing, peak heat flux decreased from 9.6 W m^{-2} (REF) to 6.3 W m^{-2} (PCM1), a 33.3% reduction. Under TN, the reduction was from 6.3 W m^{-2} to 3.8 W m^{-2} (−39.7%) and finally, under the Palermo case (named PA), it decreased from 5.9 W m^{-2} to 3.4 W m^{-2} (−42.4%). These effects were linked also to a modification of the heat flux profile, shifting from a sinusoidal pattern (REF) to a more distorted waveform (PCM1), consistent with latent heat absorption and release during phase change.

Fig. 7 displays trends of external temperature, internal heat flux, and interface heat flux between the wall and PCM, to further investigate the thermal dynamics at the PCM interface. A double-peak pattern emerged under STD and TN conditions, indicating a saturation effect of the PCM. As the temperature rose toward the material's melting point occurring in the range 23–28 °C [51], energy was first absorbed and stored (first peak), followed by a second, more pronounced peak as the PCM's storage capacity became saturated and no latent effects are present, increasing the heat flux transmitted towards the internal side. The progressive saturation effect of the phase change material during the daily heating cycle is explained by the fact that during the heating phase, the PCM undergoes melting and absorbing heat in the latent regime, temporarily limiting the heat flux transmitted through the wall and this is visible by the first peak which is characterized by an almost flat trend. Once the latent storage capacity is exhausted and the material becomes fully melted in the measured area, the buffering effect is lost and heat transfer returns predominantly in the sensible regime, causing a

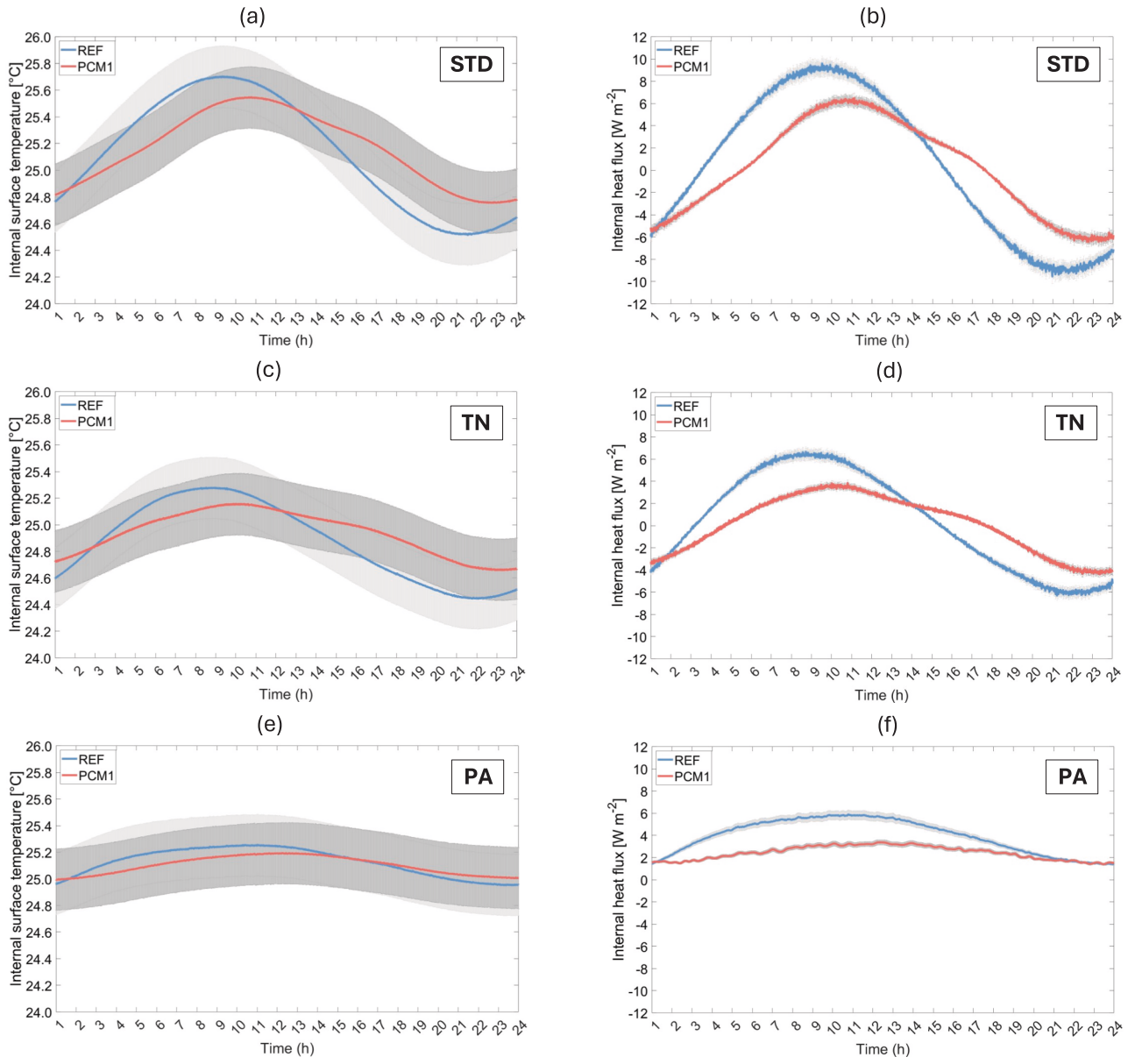

Fig. 6. Effect of a single layer of PCM of 5 mm thickness (PCM1), with respect to REF case, on either the internal surface temperature (a,c,e) and internal heat flux (b, d,f).

renewed increase in the heat flux and the appearance of a secondary peak. A symmetrical effect was observed during cooling, reflecting the solidification process. Differently from this, under the climate of Palermo this behaviour was not present since the material was always subjected at a higher average temperature close to the material's melting point.

The periodic thermal behaviour of the tested wall configurations, as summarized in Table 2, demonstrated the impact of adding a PCM layer inside the tested wall on dynamic thermal properties. The table provides a summary of the three computed key parameters, which are Δt_{ie}, Y_{ie} and f, for the three different climatic conditions.

According to Table 2, the time-shift increased consistently with the PCM integration across all scenarios. In fact, in both the STD and TN cases, the reference configuration showed a delay of 2.8 h, which extended to 4.2 h with PCM1, indicating a 50% increase in terms of heat flux delay towards the internal chamber. The PA case also showed an important increase, from 2.9 to 3.9 h, corresponding to a 35% enhancement. This consistent increase across all test conditions confirms the PCM's ability to delay the heat flux, thereby enhancing the thermal inertia of the wall. The periodic thermal transmittance values in Table 2 further emphasize the PCM's effect. In the STD condition, Y_{ie} decreased from 1.167 W m^{-2} K^{-1} (REF) to 0.808 W m^{-2} K^{-1} (PCM1), representing a 30.8% reduction. Similarly, in the TN case, the value decreased from 1.157 to 0.882 W m^{-2} K^{-1} (i.e., –23.9%). In the PA case, although the unfiltered reduction was modest (from 1.243 to 1.053 W m^{-2} K^{-1} (−15.3%)), the application of filtered data yielded a significant decrease down to 0.491 W m^{-2} K^{-1}, equivalent to a 127% attenuation with respect to the unfiltered REF value. The marked discrepancy between the original and filtered signals observed for Palermo can be attributed to the lower signal-to-noise ratio (S/N), resulting from the reduced heat flux amplitudes recorded under these boundary conditions. The lower flux magnitude increases the relative influence of noise on the signal, making the heat flux time series richer in higher-order harmonics. As a result, not only the fundamental harmonic but also higher-order components contribute to the evaluation of the periodic thermal parameter (Y_{ie}). This behaviour is particularly evident for Palermo, whereas in the cases of Trento and the standard forcing, the higher heat flux amplitudes result in a higher S/N ratio. Consequently,

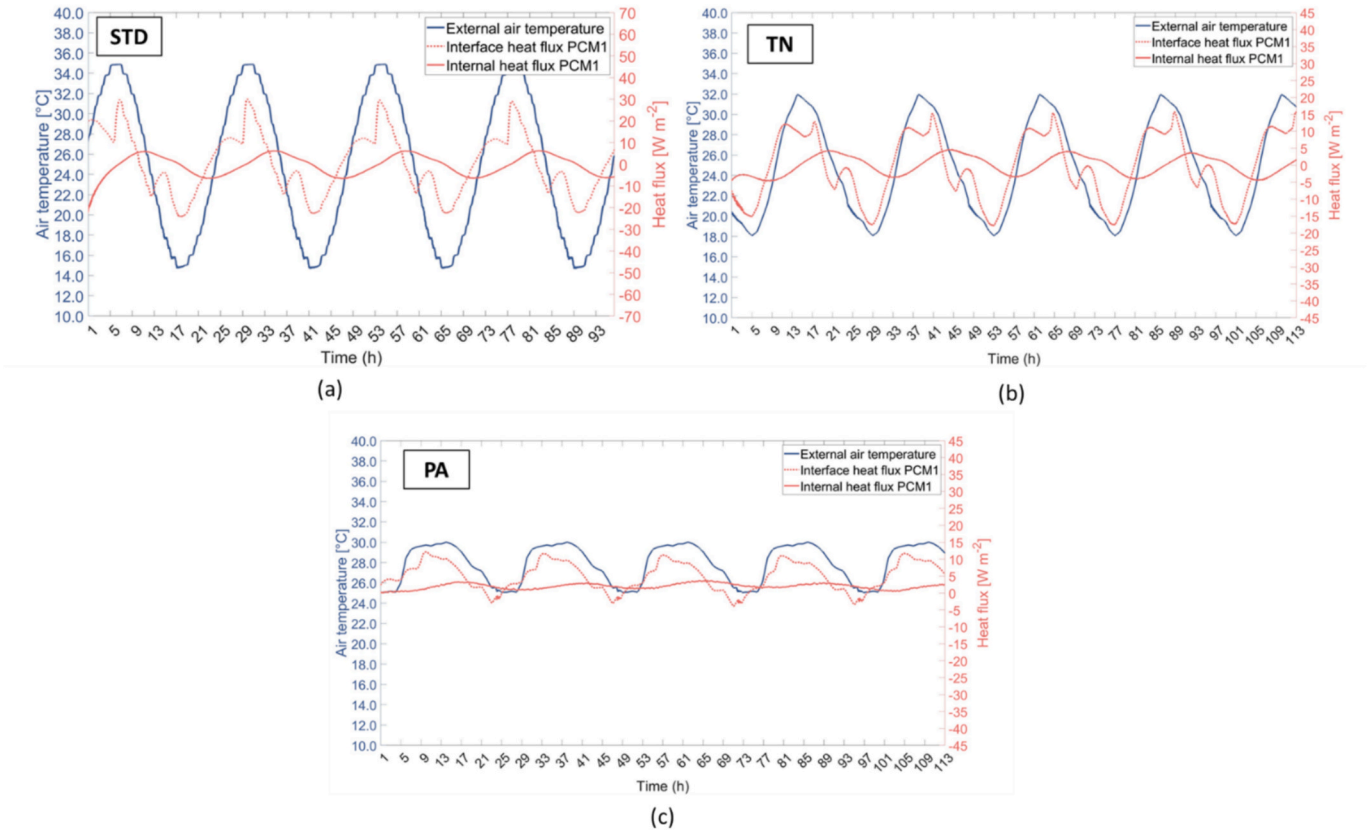

Fig. 7. External air temperature and heat flux measured at the internal side and interface for the single layer PCM1.

Table 2
Results for the PCM1 vs. REF wall with original and filtered signals.

Climate	Signal	Wall	Y_{ie} (W m^{-2} K^{-1})	Δt_{ie} (h)	f (−)
STD	Original	REF	1.167 (±14.1%)	2.2 (±0.8%)	0.744 (±11.4%)
		PCM1	0.808 (±14.1%)	3.4 (±0.6%)	0.542 (±9.2%)
	Filtered	REF	1.131	2.8	0.721
		PCM1	0.833	4.2	0.531
TN	Original	REF	1.157 (±14.4%)	3.4 (±0.6%)	0.737 (±11.5%)
		PCM1	0.882 (±14.6%)	3.4 (±0.6%)	0.592 (±9.7%)
	Filtered	REF	1.124	2.8	0.717
		PCM1	0.868	4.2	0.553
PA	Original	REF	1.243 (±17.9%)	3.2 (±0.6%)	0.792 (±14.8%)
		PCM1	1.053 (±18.6%)	4.1 (±0.7%)	0.709 (±12.8%)
	Filtered	REF	1.118	2.9	0.713
		PCM1	0.419	3.9	0.313

the relative contribution of higher-order harmonics is reduced, and the thermal parameter is predominantly governed by the fundamental component, leading to more consistent results between the original and filtered signals.

The trends in Table 2 highlight the extent to which PCM effectively moderates periodic heat flow, especially when analysed with post-processed data filtered out of the noise. At last, the decrement factor reflected a consistent reduction with PCM adoption. The STD condition pointed out a decrease from 0.744 to 0.542. Under TN conditions, the decrement factor showed a decrease from 0.737 to 0.592 while for PA f decreased from 0.792 to 0.706, and further to 0.313 with filtered data, marking a considerable drop, as described before for the periodic thermal property Y_{ie}. These values confirmed that the PCM layer not only delays thermal transmission but also dampens its magnitude, reducing heat fluxes transmitted to indoor.

Table 3 reports the energy stored in the wall (with and without PCM) per cycle. The reference wall without PCM is reported as E_{REF}, while the wall with a single layer of PCM is called E_{PCM1}. Along this, the contribution of the PCM layer in terms of stored energy is reported as $E_{st,PCM}$, computed as integral of the thermal balance only on the Phase Change Material layer. As a result of the PCM integration, the single layer increased up to more than double the initial energy storage capacitance of the wall across all temperature conditions as reported in the following table.

In order to quantify such increase, in absolute terms, STD conditions produced the highest energy storage, consistent with the greater temperature amplitude. The same was noticed under the TN forcing. In PA, the PCM's contribution was less dominant. The total stored energy increased by about 60%, but the wall component accounted for the majority. This reduced PCM effectiveness is likely due to the external temperature oscillating near the PCM's melting point, limiting phase change cycles. This means that the PCM might not return fully to its solid phase, reducing the latent heat recovery.

Table 3
Comparison of the stored energy of the reference wall without PCM (E_{REF}) and with the single PCM layer PCM1 (E_{PCM1}) expressed in Wh m^{-2} for the three different climates, standards (STD), Trento (TN) and Palermo (PA). The contribution of the PCM to the whole stored energy of the wall is reported as $E_{st,PCM}$ in Wh m^{-2}.

Forcing	E_{REF} (Wh m^{-2})	E_{PCM1} (Wh m^{-2})	$E_{st,PCM}$ (Wh m^{-2})
STD	247.3 ± 17.3	366.6 ± 25.7	212.8 ± 14.9
TN	166.8 ± 11.7	284.5 ± 19.9	186.2 ± 13.0
PA	79.8 ± 5.6	128.2 ± 9.0	44.0 ± 3.1

3.3. Impact of a double layer of phase change material

The implementation of a double layer of Phase Change Material on the external surface of the analyzed reference wall has shown negligible impact on the stationary U-value (equal to 1.144 ± 0.038 W m^{-2} K^{-1}) with respect to the single-layer configuration, with a reduction of the U-value of about 4%. However, it showed significant benefits in controlling internal heat flux under periodic boundary conditions with internal heat flux peaks reduced by more than double, as shown in Fig. 8, as well as in resulting thermal properties of the wall, as shown in Table 4. Compared to the single PCM layer configuration, the double layer setup, named PCM2, demonstrated a more pronounced effect. The measured thermal response confirmed that the PCM2 wall configuration not only reduces the amplitude of the heat flux but also shifts it strongly over time. This behavior was registered for all cases, except for the warmer one of Palermo (PA). As shown in Fig. 8, the internal heat flux peak in the reference wall under a standard (STD) sinusoidal forcing reached 9.6 W m^{-2}, which decreased to 3.4 W m^{-2} in the PCM2 configuration, which means a reduction of 6.2 W m^{-2}, corresponding to a 64.6% decrease. This reduction was nearly double in comparison to the results observed with the single layer. Furthermore, differently for the single layer case, the appreciable effect of the double layer showed influence on the internal surface temperature as well, especially during the second half of the testing period. In this phase, the temperature profile for PCM2 lied outside the error band of the reference case, confirming the greater modulation offered by the double layer. These thermal improvements were reflected in the periodic thermal parameters, reported in Table 4. Under sinusoidal conditions, the periodic thermal transmittance decreased from 1.131 W m^{-2} K^{-1} (filtered REF) to 0.449 W m^{-2} K^{-1} (filtered PCM2), i.e., a 60.3% reduction. The decrement factor dropped from 0.721 to 0.286, while the time-shift increased from 2.8 h to 6.7 h, corresponding to an enhancement of 139.3%. This confirmed the greater capacity of double PCM in shifting and shaving the heat flux entering the building. Under Trento conditions (TN), the periodic thermal transmittance decreased by 58.6%, from 1.124 W m^{-2} K^{-1} to 0.465 W m^{-2} K^{-1}. The decrement factor was reduced by 58.7%, and the time-shift increased from 2.8 h to 6.5 h (+132.1%). Similarly, the heat flux peak dropped from 6.6 W m^{-2} (REF) to 1.9 W m^{-2} (PCM2), indicating a

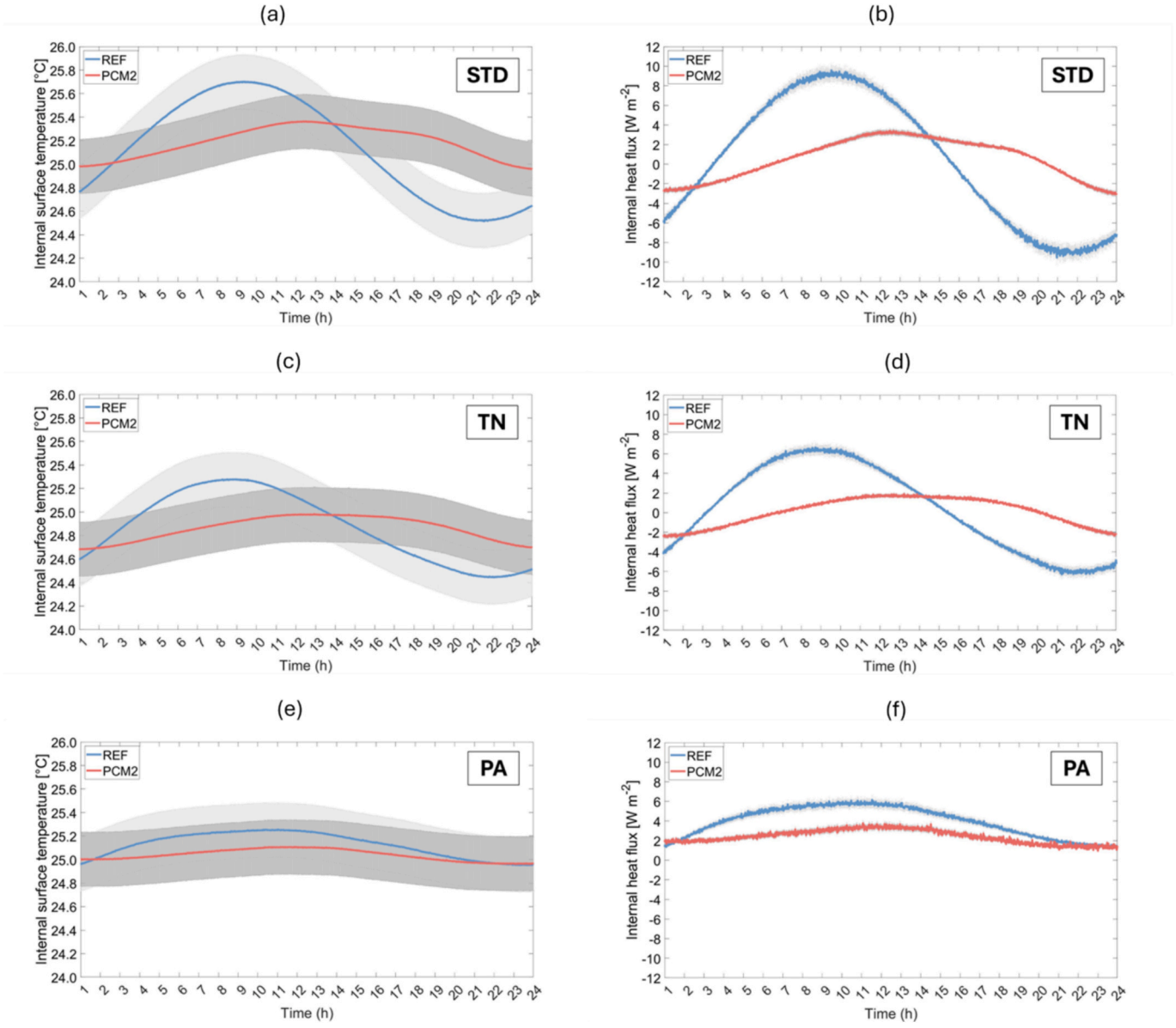

Fig. 8. Effect of a double layer of PCM of 10 mm thickness (PCM2), with respect to REF case, on either the internal surface temperature (a,c,e) and internal heat flux (b,d,f).

Table 4
Results for the PCM2 vs. REF wall with original and filtered signals.

Climate	Signal	Wall	Y_{ie} (W m^{-2} K^{-1})	Δt_{ie} (h)	f (−)
STD	Original	REF	1.167 (±14.1%)	2.2 (±0.8%)	0.744 (±11.4%)
		PCM2	0.458 (±14.1%)	5.7 (±0.3%)	0.322 (±11.0%)
	Filtered	REF	1.131	2.8	0.721
		PCM2	0.449	6.7	0.286
TN	Original	REF	1.157 (±14.4%)	3.4 (±0.6%)	0.737 (±11.5%)
		PCM2	0.455 (±14.6%)	6.2 (±0.3%)	0.320 (±11.1%)
	Filtered	REF	1.124	2.8	0.717
		PCM2	0.465	6.5	0.296
PA	Original	REF	1.243 (±17.9%)	3.2 (±0.6%)	0.792 (±14.8%)
		PCM2	0.512 (±17.9%)	2.6 (±0.7%)	0.361 (±10.7%)
	Filtered	REF	1.118	2.9	0.713
		PCM2	0.343	4.3	0.219

71.2% reduction. These values confirmed the enhanced thermal inertia offered by PCM2 in colder or temperate climates. In Palermo, the benefits of the double PCM layer were present, but less marked. The filtered Y_{ie} decreased from 1.118 to 0.343 W m^{-2} K^{-1}, corresponding to a 69.3% reduction. The decrement factor from 0.713 to 0.219, and the time-shift rise modestly from 2.9 h to 4.3 h (+48.3%). The maximum heat flux reduction was more limited: from 5.9 W m^{-2} (REF) to 3.8 W m^{-2} (PCM2), i.e., 35.6%. This attenuation reflected the reduced capacity of the PCM to undergo full phase change under warmer climates, where temperatures remain close to the PCM's melting point.

These improvements were supported by results in terms of stored energy per cycle summarized in Table 5. As for the single layer case, also here results are reported in terms of the reference wall without PCM, named as E_{REF}, while the wall with the double PCM layer is called E_{PCM2}. Along this, the contribution of the double layer in terms of stored energy is reported as $E_{st,PCM}$, computed as integral of the thermal balance just on the double layer of Phase Change Material, thus, isolating its storage effect from the whole wall. The PCM2 configuration stored 73% more energy than the REF wall under STD conditions (from 247.3 to 427.8 Wh m^{-2}). Under Trento conditions, the energy storage increase was 90.4%, and even under Palermo conditions, where PCM performance was less effective, a 40.2% increase is still observed. The PCM layer in the PCM2 configuration also exhibited quicker stabilization, behaving as a thermal buffer and further supporting passive climate control.

The heat flux variation observed during the testing period demonstrated that the PCM2 configuration effectively overcame the limitations of the single-layer setup, where saturation point was reached. This trend is clearly illustrated in Fig. 9, where the PCM2 setup showed a smoother heat transfer profile without the double-peak behavior at the maximum point, differently from the single-layer configuration. This behavior indicated that increasing the mass of the PCM material enhanced its storage capacity, as a result improving its overall thermal performance and reducing the saturation effect due to a higher active mass involved.

Table 5
Comparison of the stored energy of the reference wall without PCM (E_{REF}) and with the double PCM layer PCM2 (E_{PCM_2}) expressed in Wh m^{-2} for the three different climates, standards (STD), Trento (TN) and Palermo (PA). The contribution of the PCM to the whole stored energy of the wall is reported as $E_{st,PCM}$ in Wh m^{-2}.

Forcing	E_{REF} (Wh m^{-2})	E_{PCM2} (Wh m^{-2})	$E_{st,PCM}$ (Wh m^{-2})
STD	247.3 ± 17.3	427.8 ± 2.9	384.4 ± 26.9
TN	166.8 ± 11.7	317.6 ± 22.2	277.1 ± 19.4
PA	79.8 ± 5.6	111.9 ± 7.8	55.5 ± 3.9

The beneficial effect of using a double layer of Phase Change Material (PCM) is clearly noticed under specific climatic conditions, especially when the external temperature follows a standard seasonal profile or the one of an Alpine region such as Trento. In these scenarios, the introduction of a second PCM layer yields a marked improvement in the thermal performance of the wall. The added thermal mass and enhanced heat storage capacity contribute to better temperature regulation, leading to increased energy efficiency and possible improvements in indoor comfort. Conversely, when the same PCM configuration is applied in a warmer climate, such as the one of Palermo, advantages of a second layer are less marked, as shown in Fig. 10. In this context, the thermal conditions do not allow the PCM to undergo sufficient phase transitions, leading to its latent heat storage capacity not fully exploitable. As a result, the performance of the wall shows a plateau after the first PCM layer is added, and the addition of a second layer does not contribute to further improvements. These findings confirm that PCM performance strongly depends on the alignment between the melting temperature and the local climatic conditions, and that improved results in warm environments require a climate-specific selection of the phase-change temperature range. In this regard, the literature consistently indicates that there is no universally optimal melting temperature, but rather a suitable range that must be identified based on the interaction between climate conditions, building characteristics, and operating constraints [58–60]. For building applications, melting temperatures close to the indoor comfort range (typically 24 – 28 °C) are generally recommended, as they enable effective passive thermal regulation while ensuring regular and repeatable phase-change cycling [58,59]. In the case of Palermo, where the PCM layer is installed externally, selecting a melting temperature consistent with the outdoor temperature profile would promote more effective daily regeneration and enhanced thermal performance. However, PCM selection must ensure stable operation over the entire cooling season, rather than maximizing performance during specific short-term extreme conditions [59,60]. Although slightly higher melting temperatures could increase PCM activation during the hottest periods, the limited night-time cooling typical of warm Mediterranean climates may restrict complete solidification, thereby reducing the PCM's ability to regenerate its latent storage capacity and decreasing its overall seasonal effectiveness. Therefore, the melting temperature adopted in this study represents a balanced compromise, consistent with literature recommendations, ensuring reliable operation under realistic climatic conditions while maintaining comparability and representativeness of the results [58–60].

3.4. Energy and thermal power implications of PCM integration in building walls

The application of Phase Change Materials (PCM) within building envelope systems has demonstrated an effective capacity in temperature and thermal power peaks shaving. This section evaluates the possible benefits in terms of energy savings related to a HVAC system when PCMs are integrated inside building walls.

3.4.1. Peak power reduction

The application of PCMs at the external side of walls has demonstrated to be effective in reducing the peak of heat fluxes. Table 6 summarizes the reductions in internal peak heat flux achieved by applying a 5 mm (PCM1) and 10 mm (PCM2) PCM layer compared to the reference wall (REF) without PCM under the three tested temperature profiles.

This reduction achieved through PCM integration has a direct impact on the design and operation of HVAC systems, particularly if heat pumps are considered as heating/cooling system. The application of PCM layers can lower the instantaneous thermal load since it reduces the transmitted heat from the external building envelope to the indoor environment, especially during the warmest hours of the day. This attenuation and time-shift of thermal peaks help to flatten the cooling demand curve,

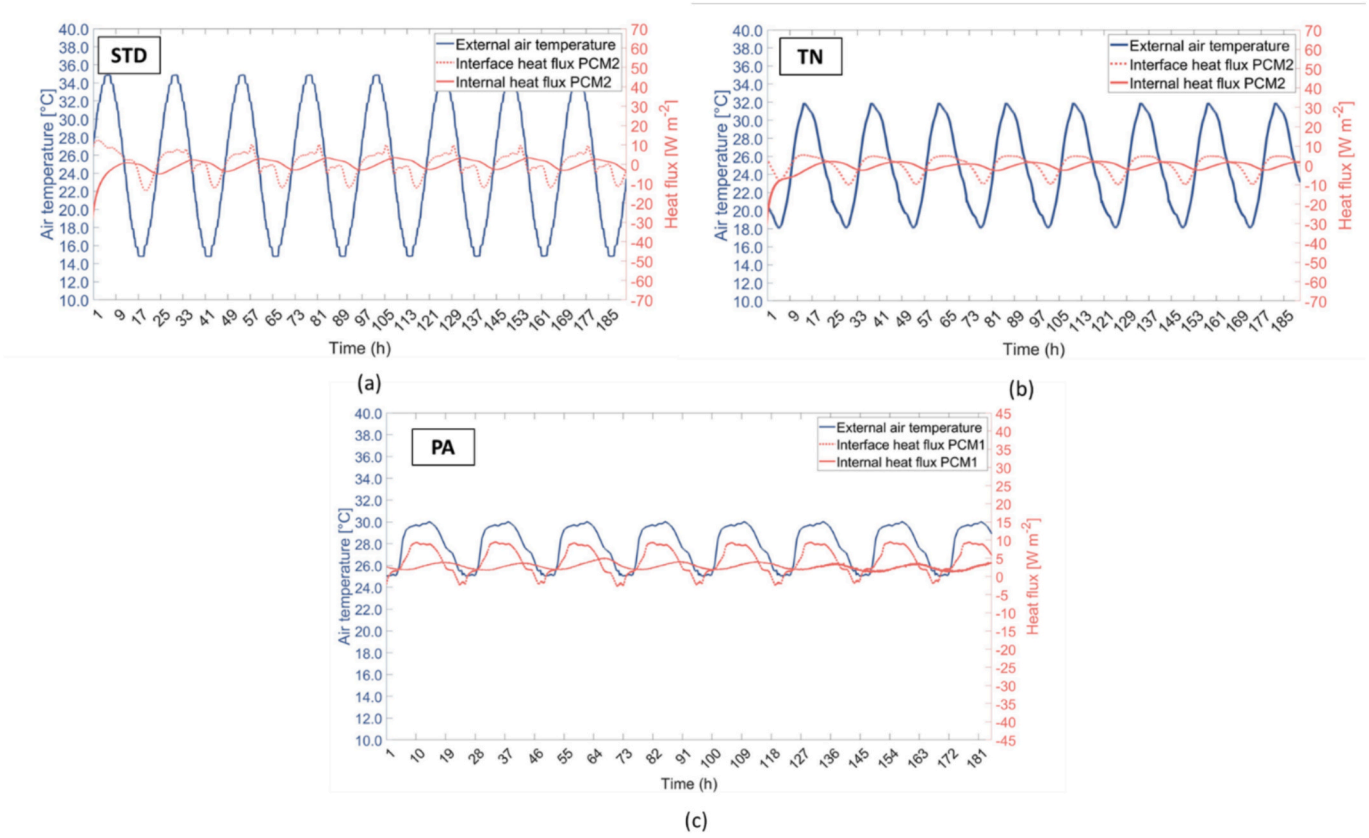

Fig. 9. External air temperature and heat flux measured at the internal side and interface for the single layer PCM2.

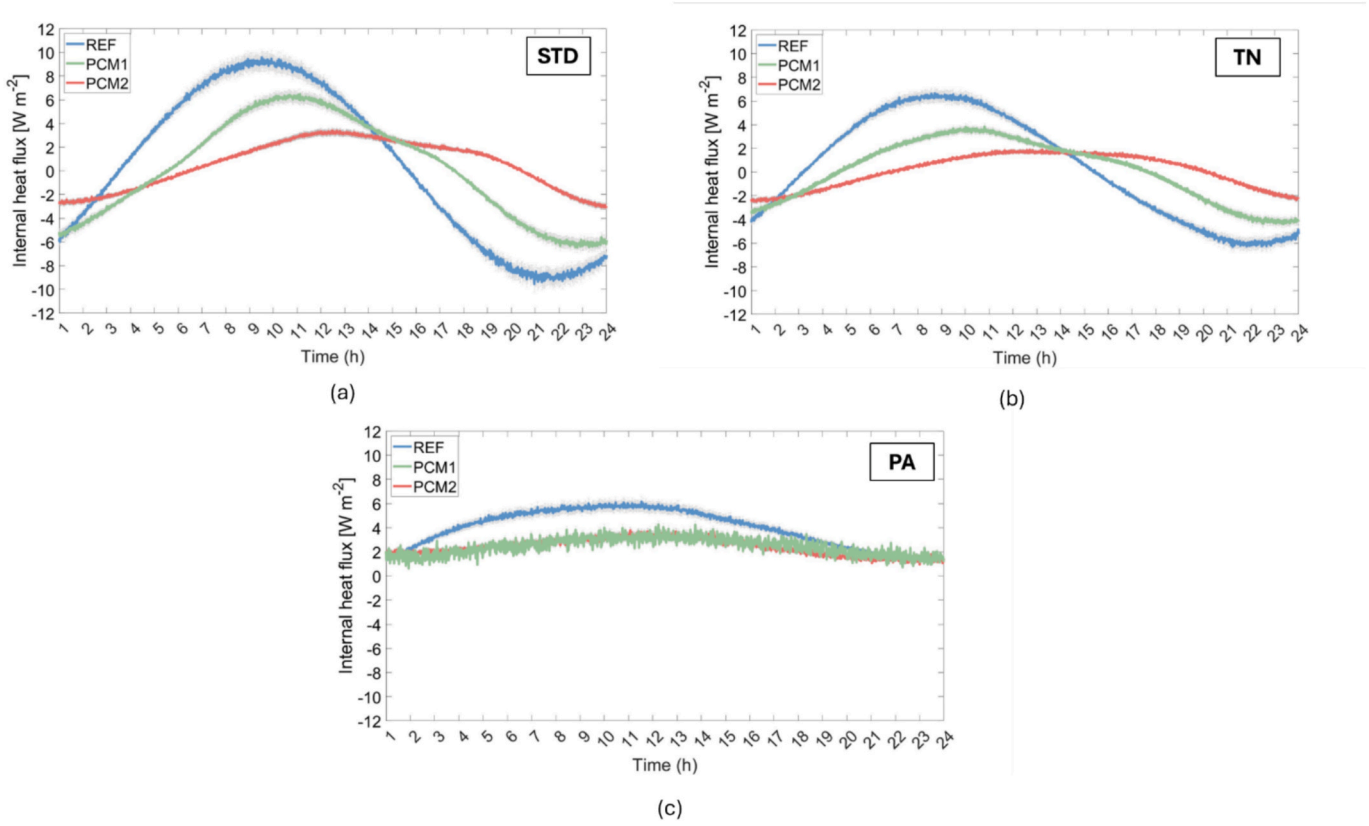

Fig. 10. Trends in internal heat flux for the wall without PCM (REF), with the single (PCM1) and double layer (PCM2).

Table 6
Heat flux peaks reduction – summary table.

Forcing Scenario	REF Peak (W m^{-2})	PCM1 Peak (W m^{-2})	Reduction (%) PCM1 vs REF	PCM2 Peak (W m^{-2})	Reduction (%) PCM2 vs REF
STD	9.6 ± 0.7	6.3 ± 0.4	–33.3%	3.4 ± 0.2	−64.6%
TN	6.3 ± 0.4	3.8 ± 0.3	−39.7%	1.9 ± 0.1	−71.2%
PA	5.9 ± 0.4	3.4 ± 0.2	−42.4%	3.8 ± 0.3	−35.6%

which can prevent oversizing of heating/cooling systems. In traditional HVAC design, peak external thermal loads are often used as the basis for sizing equipment to ensure thermal comfort under worst-case conditions. However, PCM integration can reduce the required cooling capacity, enabling the selection of smaller and often less expensive HVAC units. For this analysis, peak load reductions per unit of surface were adopted to extend results to buildings having different sizes. According to Menin et al. [61], the average cost of heat pump systems was found to be approximately 940 € per kW of thermal capacity, and such value allowed for a direct estimation of capital cost savings of the HVAC system per unit of surface covered with phase change material. By applying such correlation to the reduction of thermal peak loads obtained experimentally, savings in heat pump capital cost could be estimated (Table 7). It should be noted that the temperature profiles adopted in this study reach values close to the design outdoor temperatures for cooling defined according to the Standard EN ISO 15927–2 for the investigated locations. Therefore, the analysis provides a realistic estimation of PCM effectiveness under near-design conditions. Nevertheless, the calculated capital savings should be interpreted as an indicative estimate of the potential peak load reduction enabled by PCM integration under the current testing conditions, rather than a definitive equipment sizing recommendation.

The capital saving related to the reduced heat pump capacity can be directly compared with the actual commercial cost of PCM implementation which is equal to 84.2 € m^{-2} (single layer of 5 mm) and 168.5 € m^{-2} for the 10 mm layer according to the state of the art of this technology. Table 7 summarizes the investment costs and the capital savings for the two PCM solutions under the three climates.

Under current market conditions, it can be immediately pointed out that the PCM investment cost is extremely higher than the capital savings related to the reduction of the heat pump capacity. For instance, a maximum saving of 5.8 € per square meter of applied PCM (in the case of double PCM layer under STD boundary conditions) compared to the PCM cost per square meter which is 168.5 € when considering a double layer. This is mainly due to the higher production costs associated with a premature technology. Although numerous studies are available in the literature, the technology has not yet been investigated in a sufficiently extensive way to provide robust, consistent, and reproducible results that would support practitioners in confidently applying such materials in real-world buildings. A further consideration must be added. Achieving a flatter cooling load also reduces the variability of the heat pump's capacity ratio. This not only allows for a smaller system size but also leads to improved operating conditions. The inverter driven heat pump/chiller will operate for a larger number of hours within the modulation range, thereby reducing operation with frequent on–off cycling, which degrades the coefficient of performance and increases electrical energy consumption. If properly designed, integrating PCM within the wall can also be exploited for the implementation of advanced control strategies aimed at improving photovoltaic self-consumption. Furthermore, the availability of incentives and subsidies, such as tax credits, energy-efficiency grants, or national renovation bonuses, can help the economic viability, as well as the deployment of such technology. When combined with governmental or regional incentives, PCM adoption can become more attractive, making it a competitive and complementary solution for improving indoor comfort, managing summer cooling loads, and achieving energy efficiency in both new-build and retrofit applications. Finally, the economic comparison presented here refers primarily to the initial investment associated with equipment sizing. At this stage, the PCM system has been validated at laboratory scale, and its performance under real operating conditions has not yet been quantified. Future work will therefore involve full-scale implementation in a monitored test cell, enabling long-term assessment of energy performance and supporting a more comprehensive techno-economic evaluation.

3.4.2. *Energy demand redistribution*

While the reduction of peak cooling power represents the main outcome of PCM integration, it is equally important to highlight the effects on the temporal distribution of cooling energy demand. Lowering and delaying the maximum cooling load, it also influences the temporal distribution of the cooling demand. A total daily energy use remained nearly unchanged by considering internal heat flux profiles measured for each configuration and climate. In fact, results show net values equal to zero by integrating heat flux across the 24 h. Even if this result may seem limited, it highlights important contribution of the PCM behaviour. The way the PCM is installed in this study, thus, at the external side, allows the wall-PCM system to alter the internal heat flux profile by shifting and dampening the instantaneous energy inwards the conditioned environment. This behaviour is consistent with the periodic stabilized conditions of the tests and confirms that the PCM primarily provides load shifting and peak attenuation rather than reducing the daily integrated heat flow over the 24 h, which is the period of the applied forcing.

When shorter periods are analysed, particularly the critical 12-hour daytime interval, the scenario completely changes. The use of PCM leads to a measurable reduction in cooling demand, as well. Table 8 reports the inwards thermal energy reduction during the day when the PCM is in the absorption phase, computed as the difference between the stored energy with and without PCM integration, considering the whole wall assembly. In particular, the calculation was performed as the difference between either E_{PCM1} or E_{PCM2} and the E_{REF}, according to the analysed case.

Thermal energy reduction is more enhanced in climates with a higher external temperature variation, such as STD and TN, and this increases by doubling the PCM layer. On the contrary, in warmer climates and with a lower thermal excursion, the analysed PCM behaves poorly showing almost the same thermal energy reduction during the

Table 7
PCM investment and capital saving – summary table.

Climate	PCM Type	Peak reduction (W m^{-2})	Capital Saving (€ m^{-2})	PCM investment (€ m^{-2})
STD	PCM1	3.3	3.1	84.2
	PCM2	6.2	5.8	168.5
TN	PCM1	2.5	2.4	84.2
	PCM2	4.4	4.1	168.5
PA	PCM1	2.5	2.4	84.2
	PCM2	2.1	2.0	168.5

Table 8
Energy savings during the PCM absorption phase in the diurnal hours.

Climate	PCM Type	Thermal energy reduction (Wh m^{-2})
STD	PCM1	−119.3
	PCM2	−180.5
TN	PCM1	−117.7
	PCM2	−150.8
PA	PCM1	−48.4
	PCM2	–32.1

absorption phase. This reduction in energy during the most critical hours of the day allow the system to reduce the energy consumption of the HVAC system adopted inside the building to keep the set-point inside the conditioned environment. This behaviour is explained by the latent heat storage capacity of the material, which absorbs excess thermal energy during peak heat gains and releases it later when the external temperature decreases. By delaying and spreading the internal heat load over a longer period, the PCM reduces the intensity of cooling demand precisely when external conditions and internal gains are at their maximum. Consequently, during the day when the HVAC system would normally be intensively adopted, the demand for active cooling is reduced. Furthermore, beyond the direct energy reduction during this active period, the temporal redistribution of the heat flux can have additional advantages like aligning the cooling demand more closely with hours of the day when there are potentially lower electricity costs and it can facilitate the integration of renewable energy sources by shifting loads. Moreover, in some climate conditions with high thermal excursion between day and night (such as TN and STD) the use of PCM may allow to dissipate heat during the night period by natural or forced ventilation with external air without air conditioning.

3.4.3. Implications for building operation

The adoption of PCM in building envelopes therefore seems providing a dual benefit. On one hand, it acts as a peak attenuator by lowering the maximum cooling power required. This has direct consequences for HVAC system sizing, since smaller peak demands can allow for a reduced equipment size and potentially lower initial investment costs. On the other hand, PCM works as a load shifting mechanism by moving part of the cooling demand to less critical hours, which improves the match between building needs and system availability. For building operation, this dual effect is particularly important. Reduced peak loads not only enhance the operational efficiency of HVAC systems but they can also improve occupant thermal comfort by minimizing fast variations of indoor ambient conditions. Furthermore, the load-shifting capacity of PCM can help in the development of demand-side management strategies, making buildings more resilient to external solicitation, e.g., such as heat waves. Finally, from an economic point of view, redistributing the cooling demand away from high-costs hours can reduce operating costs.

4. Conclusions

This research confirms that the use of elastomeric panels containing Phase Change Materials (PCMs) can be a promising solution for improving thermal performance in building envelopes, especially in summer seasons. Through a comprehensive experimental campaign on real-scale wall configurations, clear benefits were observed in terms of thermal power required for the cooling process, as well as thermal energy reductions during the absorption phase of the PCM. Specifically, the integration of PCMs led to a substantial reduction of the heat flux peak entering the conditioned environment, as well as a significant shift in time. These effects were especially pronounced under boundary conditions with strong diurnal temperature variations. Quantitatively, results showed peak heat flux reductions exceeding up to 64.6% and time-shift increases over 100% in specific configurations. Additionally, the thermal energy storage capacity of the walls was notably enhanced, confirming the PCM's ability to absorb, store, and gradually release heat. This behaviour contributes to reducing and delaying the heat propagation, a key goal for passive cooling strategies and improved indoor thermal comfort. From the energy point of view and under the current boundary conditions applied in this study, when focusing on the most critical hours of the day when the HVAC system performs the cooling, thermal energy reductions up to −180.5 Wh per square meter of PCM material were registered in a 24 h cycle.

While the current prices of PCM materials limit their widespread, also the technical contributions show results that often are not systematically obtained and less reproducible, leading to a weaker knowledge on such materials. The presented study not only proposes a preliminary systematic experimental procedure to assess the thermal behaviour of walls integrated with PCMs under different real climates, but it also increases the current literature and the data base related to PCM thermal performance. Future developments of the current study will focus on in-situ seasonal evaluations involving full-scale prototypes equipped with HVAC systems. Such studies will allow for the assessment of not only thermal behaviour, but also actual savings, interaction with active systems, and overall building performance, overcoming the issue of real buildings monitoring where the only effect of the PCM cannot be isolated. Simultaneously, PCM materials should be diversified to suit different climatic zones by tuning their phase transition temperatures to the specific thermal profiles of each region. This climate-specific approach will maximize the benefits of PCM use across different geographical contexts. Equally important is the need to improve market readiness of PCM systems. Developing easy-to-handle and rapidly installable solutions will facilitate integration into both new constructions and existing buildings. Enhancing compatibility with standard wall components and construction practices can further streamline their integration. Such improvements can overcome the cost issue in the near future. By increasing PCM knowledge and reliability inside buildings, a possible industrial-scale production of PCM components, coupled with modular and prefabricated installation approaches, would reduce material's costs. Furthermore, the implementation of public incentives or financial supports for refurbishments could play a decisive role in accelerating their adoption, particularly in the residential sector and in large-scale retrofitting procedures. In conclusion, PCMs offer substantial potential to enhance the thermal inertia of building envelopes and reduce summer cooling loads. With ongoing research, technological advancements, and supportive policy frameworks, these materials are promising in contributing to future energy-efficient building designs and sustainable climate adaptation strategies.

CRediT authorship contribution statement

Maja Danovska: Writing – original draft, Methodology, Investigation, Data curation, Conceptualization. **Francesco Valentini:** Writing – original draft, Methodology, Investigation, Data curation, Conceptualization. **Maurizio Grigiante:** Writing – review & editing, Methodology. **Luca Fambri:** Writing – review & editing. **Andrea Dorigato:** Writing – review & editing. **Alessandro Prada:** Writing – review & editing, Methodology. **Alessandro Pegoretti:** Writing – review & editing.

Declaration of competing interest

The authors declare that they have no known competing financial interests or personal relationships that could have appeared to influence the work reported in this paper.

Acknowledgments

This work was partially funded by Fondazione per la Valorizzazione della Ricerca Trentina (Italy) through "Contributo Fondazione VRT".

Data availability

Data will be made available on request.

References

[1] International Energy Agency, Transition to Sustainable buildings: strategies and Opportunities to 2050, Access year 2025, Journal (issue) (2013), https://www.iea.org/reports/transition-to-sustainable-buildings.
[2] U. Berardi, A cross-country comparison of the building energy consumptions and their trends, Resour. Conserv. Recycl. 123 (2017) 230–241, https://doi.org/10.1016/j.resconrec.2016.03.014.

[3] H. Wan, T. Cao, Y. Hwang, et al., A comprehensive review of life cycle climate performance (LCCP) for air conditioning systems, Int. J. Refrig 130 (2021) 187–198, https://doi.org/10.1016/j.ijrefrig.2021.04.033.

[4] L. Xu, L. Dai, L. Yin, et al., Research on the climate response of variable thermo-physical property building envelopes: a literature review, Energ. Buildings 226 (2020) 110398, https://doi.org/10.1016/j.enbuild.2020.110398.

[5] M.K. Anser, A.A. Nassani, K.M. Al-Aiban, et al., Urban heat islands and energy consumption patterns: evaluating renewable energy strategies for a sustainable future, Energy Rep. 13 (2025) 3760–3772, https://doi.org/10.1016/j.egyr.2025.03.033.

[6] R.K. Sharma, A. Kumar, D. Rakshit, A phase change material (PCM) based novel retrofitting approach in the air conditioning system to reduce building energy demand, Appl. Therm. Eng. 238 (2024) 121872, https://doi.org/10.1016/j.applthermaleng.2023.121872.

[7] L. Cavicchia, H. von Storch, S. Gualdi, Mediterranean Tropical-like Cyclones in present and Future climate, J. Clim. 27 (19) (2014) 7493–7501, https://doi.org/10.1175/JCLI-D-14-00339.1.

[8] Provincia Autonoma di Trento. (2021). Piano Energetico Ambientale Provinciale 2021–2030 (PEAP). Retrieved from https://www.provincia.tn.it Accessed year 2025.

[9] International Energy Agency (2021). Net Zero by 2050. Journal (Issue). Access year 2025.

[10] M. Haller, S. Ludig, N. Bauer, Decarbonization scenarios for the EU and MENA power system: considering spatial distribution and short term dynamics of renewable generation, Energy Policy 47 (2012) 282–290, https://doi.org/10.1016/j.enpol.2012.04.069.

[11] European Commission. REPowerEU. 2023 02/02/2024]; Available from: https://commission.europa.eu/strategy-and-policy/priorities-2019-2024/european-green-deal/repowereu-affordable-secure-and-sustainable-energy-europe_it. Access year 2025.

[12] International Energy Agency. RePowerEU Plan : Joint European action on renewable energy and energy efficiency. 2023 02/02/2024]; Available from: https://www.iea.org/policies/15691-repowereu-plan-joint-european-action-on-renewable-energy-and-energy-efficiency. Access year 2025.

[13] M. Arıcı, F. Bilgin, S. Nižetić, H. Karabay, PCM integrated to external building walls: an optimization study on maximum activation of latent heat, Appl. Therm. Eng. 165 (2020) 114560, https://doi.org/10.1016/j.applthermaleng.2019.114560.

[14] B. He, V. Martin, F. Setterwall, Phase transition temperature ranges and storage density of paraffin wax phase change materials, Energy 29 (11) (2004) 1785–1804, https://doi.org/10.1016/j.energy.2004.03.002.

[15] D. Kumar, M. Alam, J. Sanjayan, et al., Comparative analysis of form-stable phase change material integrated concrete panels for building envelopes, Case Stud. Constr. Mater. 18 (2023) e01737, https://doi.org/10.1016/j.cscm.2022.e01737.

[16] A. Adesina, Use of phase change materials in concrete: current challenges, Renewable Energy Environ. Sustainability 4 (2019) 30, https://doi.org/10.1051/rees/2019006.

[17] A. D'Alessandro, A.L. Pisello, C. Fabiani, et al., Multifunctional smart concretes with novel phase change materials: Mechanical and thermo-energy investigation, Appl. Energy 212 (2018) 1448–1461, https://doi.org/10.1016/j.apenergy.2018.01.014.

[18] L.F. Cabeza, C. Castellón, M. Nogués, M. Medrano, et al., Use of microencapsulated PCM in concrete walls for energy savings, Energ. Buildings 39 (2007) 113–119, https://doi.org/10.1016/j.enbuild.2006.03.030.

[19] A. Castell, I. Martorell, M. Medrano, et al., Experimental study of using PCM in brick constructive solutions for passive cooling, Energ. Buildings 42 (4) (2010) 534–540, https://doi.org/10.1016/j.enbuild.2009.10.022.

[20] X. Wang, H. Yu, L. Li, et al., Experimental assessment on the use of phase change materials (PCMs)-bricks in the exterior wall of a full-scale room, Energy Convers. Manage. 120 (2016) 81–89, https://doi.org/10.1016/j.enconman.2016.04.065.

[21] P. Sukontasukkul, T. Sutthiphasilp, W. Chalodhorn, et al., Improving thermal properties of exterior plastering mortars with phase change materials with different melting temperatures: paraffin and polyethylene glycol, Adv. Build. Energy Res. 13 (2) (2019) 220–240, https://doi.org/10.1080/17512549.2018.1488614.

[22] M. Kheradmand, M. Azenha, J.L.B. de Aguiar, et al., Experimental and numerical studies of hybrid PCM embedded in plastering mortar for enhanced thermal behaviour of buildings, Energy 94 (2016) 250–261, https://doi.org/10.1016/j.energy.2015.10.131.

[23] M.J. Abden, Z. Tao, Z. Pan, et al., Inclusion of methyl stearate/diatomite composite in gypsum board ceiling for building energy conservation, Appl. Energy 259 (2020) 114113, https://doi.org/10.1016/j.apenergy.2019.114113.

[24] W. Li, M. Rahim, D. Wu, M. El Ganaoui, R. Bennacer, Dynamic integration of phase change material in walls for enhancing building thermal performance – a novel self-adaptive method for moving PCM layer, Energ. Conver. Manage. 308 (2024) 118401, https://doi.org/10.1016/j.enconman.2024.118401.

[25] R. Ansuini, R. Larghetti, A. Giretti, et al., Radiant floors integrated with PCM for indoor temperature control, Energ. Buildings 43 (11) (2011) 3019–3026, https://doi.org/10.1016/j.enbuild.2011.07.018.

[26] A.K. Athienitis, C. Liu, D. Hawes, D. Banu, D. Feldman, Investigation of the thermal performance of a passive solar test-room with wall latent heat storage, Energ. Buildings 32 (1997) 405–410, https://doi.org/10.1016/S0360-1323(97)00009-7.

[27] J. Yu, H. Yang, J. Zhao, et al., Study on thermal performance of dynamic insulation roof integrated with phase change material, Energ. Buildings 303 (2024) 113832, https://doi.org/10.1016/j.enbuild.2023.113832.

[28] Q. Al-Yasiri, A.K. Alshara, M.A. Sudani, et al., Advanced building envelope by integrating phase change material into a double-pane window at various orientations, Energ. Buildings 328 (2025) 115140, https://doi.org/10.1016/j.enbuild.2024.115140.

[29] R. Kumar, S. Singh, A. Dixit, Temperature-history method for characterizing thermophysical properties of phase change materials: a critical review, J. Therm. Anal. Calorim. 150 (3) (2025) 1445–1475, https://doi.org/10.1007/s10973-024-13874-2.

[30] R. Baetens, B.P. Jelle, A. Gustavsen, Phase change materials for building applications: a state-of-the-art review, Journal of Energy and Buildings 42 (9) (2010) 1361–1368, https://doi.org/10.1016/j.enbuild.2010.03.026.

[31] L. Navarro, A. de Gracia, D. Niall, et al., Thermal energy storage in building integrated thermal systems: a review. Part 2, Integration as Passive System. Renewable Energy 85 (2016) 1334–1356, https://doi.org/10.1016/j.renene.2015.06.064.

[32] L.F. Cabeza, A. Castell, C. Barreneche, et al., Materials used as PCM in thermal energy storage in buildings: a review, Renew. Sustain. Energy Rev. 15 (3) (2011) 1675–1695, https://doi.org/10.1016/j.rser.2010.11.018.

[33] Z. Pavlík, J. Fořt, M. Pavlíková, et al., Modified lime-cement plasters with enhanced thermal and hygric storage capacity for moderation of interior climate, Energ. Buildings 126 (2016) 113–127, https://doi.org/10.1016/j.enbuild.2016.05.004.

[34] M.I. Nizovtsev, A.N. Sterlyagov, Effect of phase change material (PCM) on thermal inertia of walls in lightweight buildings, Journal of Building Engineering 82 (2024) 107912, https://doi.org/10.1016/j.jobe.2023.107912.

[35] A. Ahmad, S.A. Memon, H. Dang, et al., Breaking new ground: a first-of-its-kind critical analysis of review articles on phase change materials for building applications, Appl. Energy 392 (2025) 125984, https://doi.org/10.1016/j.apenergy.2025.125984.

[36] M. Faraji, Numerical computation of solar heat storage in phase change material/concrete wall, Int. J. Energy Environ. 5 (3) (2014) 353–360.

[37] X. Jin, M.A. Medina, X. Zhang, Numerical analysis for the optimal location of a thin PCM layer in frame walls, Appl. Therm. Eng. 103 (2016) 1057–1063, https://doi.org/10.1016/j.applthermaleng.2016.04.056.

[38] Q. Wang, R. Wu, Y. Wu, C.Y. Zhao, Parametric analysis of using PCM walls for heating loads reduction, Energ. Buildings 172 (2018) 328–336, https://doi.org/10.1016/j.enbuild.2018.05.012.

[39] P. Marín, M. Saffari, A.D. Gracia, X. Zhu, M.M. Farid, L.F. Cabeza, S. Ushak, Energy savings due to the use of PCM for relocatable lightweight buildings passive heating and cooling in different weather conditions, Energ. Buildings 129 (2016) 274–283, https://doi.org/10.1016/j.enbuild.2016.08.007.

[40] F. Kuznik, J. Virgone, J. Noël, Optimization of a phase change material wallboard for building use, Appl. Therm. Eng. 28 (2008) 1291–1298, https://doi.org/10.1016/j.applthermaleng.2007.10.012.

[41] A. Figueiredo, R. Vicente, J. Lapa, C. Cardoso, F. Rodrigues, J. Kämpf, Indoor thermal comfort assessment using different constructive solutions incorporating PCM, Appl. Energy 208 (2017) 1208–1221, https://doi.org/10.1016/j.apenergy.2017.09.032.

[42] C.K. Halford, R.F. Boehm, Modeling of phase change material peak load shifting, Energ. Buildings 39 (2007) 298–305, https://doi.org/10.1016/j.enbuild.2006.07.005.

[43] Y. Cascone, A. Capozzoli, M. Perino, Optimisation analysis of PCM-enhanced opaque building envelope components for the energy retrofitting of office buildings in Mediterranean climates, Appl. Energy 211 (2018) 929–953, https://doi.org/10.1016/j.apenergy.2017.11.081.

[44] E. Elnajjar, Using PCM embedded in building material for thermal management: Performance assessment study, Energ. Buildings 151 (2017) 28–34, https://doi.org/10.1016/j.enbuild.2017.06.010.

[45] W. Li, M. Rahim, D. Wu, et al., Dynamic integration of phase change material in walls for enhancing building thermal performance–a novel self-adaptive method for moving PCM layer, Energ. Conver. Manage. 308 (2024) 118401, https://doi.org/10.1016/j.enconman.2024.118401.

[46] F. Guarino, A. Athienitis, M. Cellura, D. Bastien, PCM thermal storage design in buildings: Experimental studies and applications to solaria in cold climates, Appl. Energy 185 (1) (2017) 95–106, https://doi.org/10.1016/j.apenergy.2016.10.046.

[47] H. Ye, L. Long, H. Zhang, R. Zou, The performance evaluation of shape-stabilized phase change materials in building applications using energy saving index, Appl. Energy 113 (2014) 1118–1126, https://doi.org/10.1016/j.apenergy.2013.08.067.

[48] M. Vega, P.E. Marín, S. Ushak, et al., Research trends and gaps in experimental applications of phase change materials integrated in buildings, J. Storage Mater. 75 (2024) 109746, https://doi.org/10.1016/j.est.2023.109746.

[49] F. Chebli, F. Mechighel, Phase change materials: classification, use, phase transitions, and heat transfer enhancement techniques: a comprehensive review, J. Therm. Anal. Calorim. 150 (3) (2025) 1353–1411, https://doi.org/10.1007/s10973-024-13877-z.

[50] F. Valentini, M. Grigiante, A. Prada, et al., Experimental dynamic thermal properties determination of EPDM/NBR panels with a shape stabilized phase Change Material based on summer daily temperatures of four cities in Italy, Energ. Buildings 318 (2024), https://doi.org/10.1016/j.enbuild.2024.114503.

[51] F. Valentini, A. Dorigato, L. Fambri, et al., Production and characterization of novel EPDM/NBR panels with paraffin for potential thermal energy storage applications, Therm. Sci. Eng. Prog. 32 (2022), https://doi.org/10.1016/j.tsep.2022.101309.

[52] CEN European committee for Standardization. (2000). EN ISO 1934. Thermal performance of buildings - Determination of thermal resistance by hot box method using heat flow meter - Masonry.

[53] European Committee for Standardization. (2018). Thermal performance of building components – Dynamic thermal characteristics – Calculation methods (EN ISO Standard No. 13786:2018). CEN.
[54] CEN European committee for Standardization. (2018). EN ISO 6946. Building components and building elements — Thermal resistance and thermal transmittance — Calculation methods.
[55] Nicholas, J.V., White, D.R. (2001). Traceable Temperatures. An Introduction to Temperature Measurement and Calibration. Second Edition. Wiley.
[56] Corrado, V., Ballarini, I., & Corgnati, S. P. (2012). National scientific report on the TABULA activities in Italy. Politecnico di Torino – Dipartimento Energia.
[57] Fast Fourier Transform. Retrieved from: https://it.mathworks.com/help/matlab/ref/fft.html Accessed year 2025.
[58] A. Halimov, J. Akhatov, Z. Iskandarov, Optimization of phase change material properties for enhanced thermal performance in building envelopes, Appl. Solar Energy 60 (4) (2024) 636–648, https://doi.org/10.3103/S0003701X22600424.
[59] K.A.R. Ismail, F.A.M. Lino, M. Teggar, M. Arıcı, P.L.O. Machado, T.A. Alves, A.C. O. De Paula, A. Benhorma, A comprehensive review on phase change materials and applications in buildings and components, ASME Open Journal of Engineering 1 (2022) 011049, https://doi.org/10.1115/1.4055185.
[60] Solgi, E., Fernando, R., & Hamedani, Z. (2019). Experimental and numerical investigations on optimal phase change material melting temperature utilized either alone or with night ventilation. In Proceedings of the 16th IBPSA International Conference and Exhibition (Building Simulation 2019), Rome, Italy.
[61] L. Menin, G. Borelli, A. Prada, G. Pernigotto, A. Gasparella, M. Baratieri, Decarbonization of space heating in the Italian Alpine context: Thermo-economic assessment of the levelized energy cost of heating under alternative renewable scenarios, Energy Convers. Manage.: X 25 (2025) 100886, https://doi.org/10.1016/j.ecmx.2025.100886.
[62] Rubitherm Technologies GmbH. (2020, October 9). RT28HC data sheet (Version 09.10.2020). chrome-extension://efaidnbmnnnibpcajpcglclefindmkaj/https://www.rubitherm.eu/media/products/datasheets/Techdata_-RT28HC_EN_09102020.PDF. Accessed in December 2026.